An Investigation of Wave Propagation Modes on a Conductor in High Frequencies

Takashi ASADA*, Yoshiko MIYAMOTO*, Akihiro AMETANI*, Naoto NAGAOKA*, Yoshihiro BABA*

This paper investigates the characteristics of wave propagation modes on a conductor in high frequencies when a pulse-like voltage is applied to the sending end, based on a finite-difference time-domain (FDTD) method of a numerical electromagnetic analysis. It is found that transition of the wave propagation mode between TEM and TM occurs at the sending and receiving ends on an insulated conductor of which the relative permittivity ε_i of the insulator is different from that of air, i.e. $\varepsilon_i \neq 1$, while only the TEM mode appears in the in the middle of the conductor. The transition is dependent on the distance from the conductor center.

1. Introduction

The earth-return impedance of power transmission line is essential to analyze phenomena on the line in a power system. Pollaczek [1] and Carson [2] derived impedance formulas separately in Germany and USA in 1928 which were identical. Later Sunde also derived a formula [3] which is different from Pollaczek's and Carson's one. Pollaczek's and Carson's has been said not applicable to high frequencies. To apply Carson's formula to the high frequencies, Wise modified Cason's fomula [4].

In 1934, Wise derived the earth-return admittance of an overhead line [5]. Although the earth-return admittance is the other essential parameter to analyze phenomena on the line, it is neglected and the space admittance which assumes a perfectly conducting earth has been used in most cases.

In 1957, Kikuchi derived general fomulas [6] of the earth-return impedance and admittance which cover all the previous formulas. By applying the formulas, he studied wave propagation characteristics on an overhead line and found transition of TEM (transverse electromagnetic) mode and TM (transverse magnetic) /TE (transverse electric) mode propagation in a high frequency region [7]. The transition had been predicted by Goubou [8,9] based on a theory of Sommerfeld [10], and it is called "Sommerfeld-Goubau" propagation by Kikuchi.

This paper investigates Sommerfeld-Gaubau propagation based on FDTD (finite-differrence time-domain) simulations. At first, Sommerfeld-Goubou propagation is explained based on the frequency response of attenuation on a single overhead conductor calculated by the earth-return impedance [11,12] and the earth-return admittance [5,13]. Then, transient responses of electric and magnetic field strength along a conductor are calculated by the VSTL [14] which is based on the FDTD method, when a step-like voltage is applied to the sending end of the conductor. From the calculated results, wave propagation mode is estimated at the both ends and the center of the conductor around the conductor.

*Faculty of Science and Engineering, Doshisha University ,Kyoto
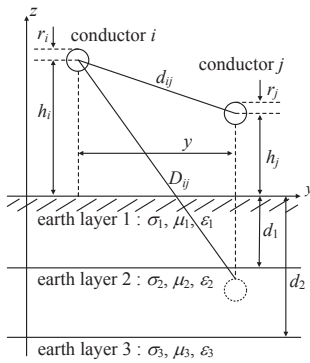Telephone: +81-744-65-6337, E-mail: dun0306@mail4.doshisha.ac.jp, ybaba@mail.doshisha.ac.jp
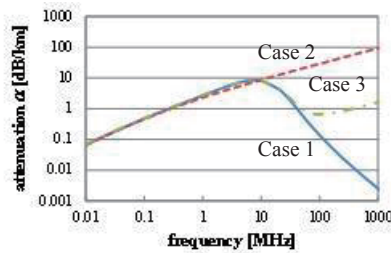
Fig. 1. An overhead two-conductor system.

Case 1: $\rho_e \neq 0$, Case 2: $\rho_e = 0$,

Case 3: with conductor internal impedance

Fig. 2. Frequency characteristic of attenuation

considering the earth-return admittance. :

$r = 1[cm]$, $h = 10[m]$, $\rho_e = 100[\Omega m]$.

2.   Sommerfeld–Goubau Propagation

Fig. 1 illustrates an overhead conductor above an earth. Fig. 2 shows the frequency characteristic of attenuation constant in the case of the earth relative permittivity being 1. The details of the earth-return impedance and admittance are described in appendix.

The solid line (case 1) in the figure is the case considering Wise's admittance in (A.10), while the dotted line (case 2) is the case of a conventional admittance given only by P_0 in (A.10) assuming a perfectly conducting earth. It is observed that α is the same in both cases in a low frequency region. Then, the attenuation when considering the earth-return admittance becomes greater than that in the conventional admittance case. At a certain frequency, the attenuation starts to decrease. The frequency is the same as the critical

frequency f_c at which the imaginary part N of the admittance in (A.10) becomes negative and the conductance G becomes negative. When the conductor internal impedance is considered (case 3), the attenuation increases again.

From the above observation, it should be clear that the earth-return admittance due to an imperfectly conducting earth affects the attenuation on a conductor. If an earth is assumed perfectly conducting as in most studies of wave propagation and transient characteristics on transmission lines and cables, the attenuation increases monotonously as frequency increases. When a real earth, which is imperfectly conducting, is considered, the attenuation starts to decrease at the critical frequency f_c. This frequency region is called "Sommefeld-Goubau propagation region", by Kikuchi, where transition occurs between TEM mode propagation (earth-return wave) and TM mode propagation (surface wave) [6,9], or it is said that displacement currents become dominant over conduction currents in air, i.e. in an insulating material.

3.   FDTD simulation

3.1.   *Model circuit*

Fig. 3 illustrates a model circuit for an FDTD simulation. A conductor is with radius $r_1 = 1$ mm and is covered by an insulator with radius $r_2 = 3$ mm and relative permittivity ε_i. Table 1 gives the FDTD simulation conditions. In the table, ρ_e, ε_r and h are the earth resistivity, the relative permittivity and the height of the conductor from the earth surface. The length of the conductor is 100 cm and is grounded through a matching resistance at the receiving end. Fig. 4 illustrates an analytical space corresponding to Fig. 3 for an FDTD simulation with cell size $\Delta s = 1$ mm. The absorbing boundary with instability-preventing coefficient $\alpha = 0.01$. Fig. 5 shows an applied current waveform with rise time 10ns at the sending end of the conductor.
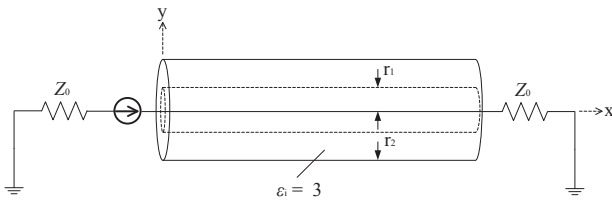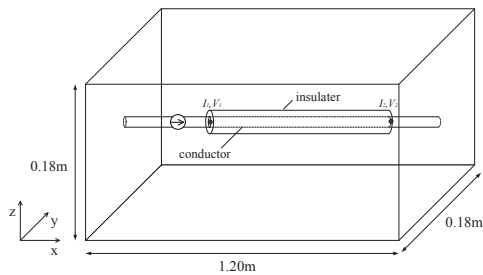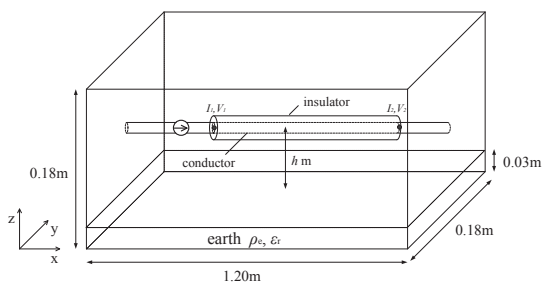
Fig. 3. A model circuit.

Table 1. Simulation conditions.

case	cable	ground		h [cm]
	ε_i	ρ [Ωm]	ε_r	
case 1	1	-	-	-
case 2	3	-	-	-
case 3	1	0	1	6
case 4	3	0	1	6
case 5	1	100	1	6
case 6	3	100	1	6
case 7	1	100	10	6
case 8	3	100	10	6
case 9	1	2000	1	6
case 10	3	2000	1	6

(a) Conductor in a free space

(b) Conductor above the earth surface

Fig. 4. Analytical space for an FDTD simulation.

3.2. Simulation results

3.2.1. Conductor in a free space : Cases 1 and 2

Figs.6 to 8 show transient responses of voltage and current, electric field and magnetic field intensities at
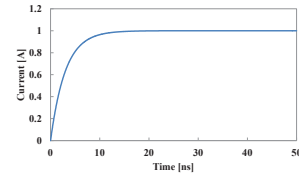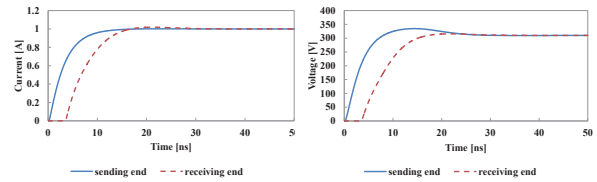

Fig. 5. Applied current waveform with T_f = 10 ns.

(a) Current   (b) Voltage

Fig. 6. Voltage and current : Case 1

Table 2. Simulation results.

x [cm]	y [mm]	case 1	case 2	case 3	case 4	case 5	case 6	case 7	case 8	case 9	case 10
0	3		TM		TM		TM		TM		TM
	13	TEM		TEM		TEM		TEM		TEM	
	23		TEM		TEM		TEM		TEM		TEM
	53										TEM
50	3										
	13	TEM	TEM	TEM	TEM	TEM	TEM	TEM	TEM	TEM	TEM
	23										
	53										
100	3		TM		TM		TM		TM		TM
	13	TEM		TEM		TEM		TEM		TEM	
	23		TEM		TEM		TEM		TEM		TEM
	53										TEM

various position, when a conductor is in a free space as in Fig. 4(a) and the relative permittivity ε_i of the insulator is 1, i.e. the same as that of the air.

It is observed that the current waveform I_2 at the receiving end is nearly the same as that I_1 at the sending end except the traveling time $t = x/c_0$ = 0.33ns in Fig. 6(a).The voltage waveform V_2 at the receiving end satisfies the relation $V_2 = Z_0 I_2$ where Z_0 is the matching impedance (resistance) as illustrated in Fig.3. The sending end voltage increase until about t = 15ns, and then decreses. For t greater than about 23ns, V_1 becomes identical to V_2 which satisfies $V = Z_0 I$, i.e. Ohm's law. The voltage increase/decrease for $0 \leqq t < 23$ ns is estimated to be caused by reflection of a traveling wave from the absorbing boundary at the both ends of the conductor. From the observation, it can be said that the wave propagation mode along the conductor in a free
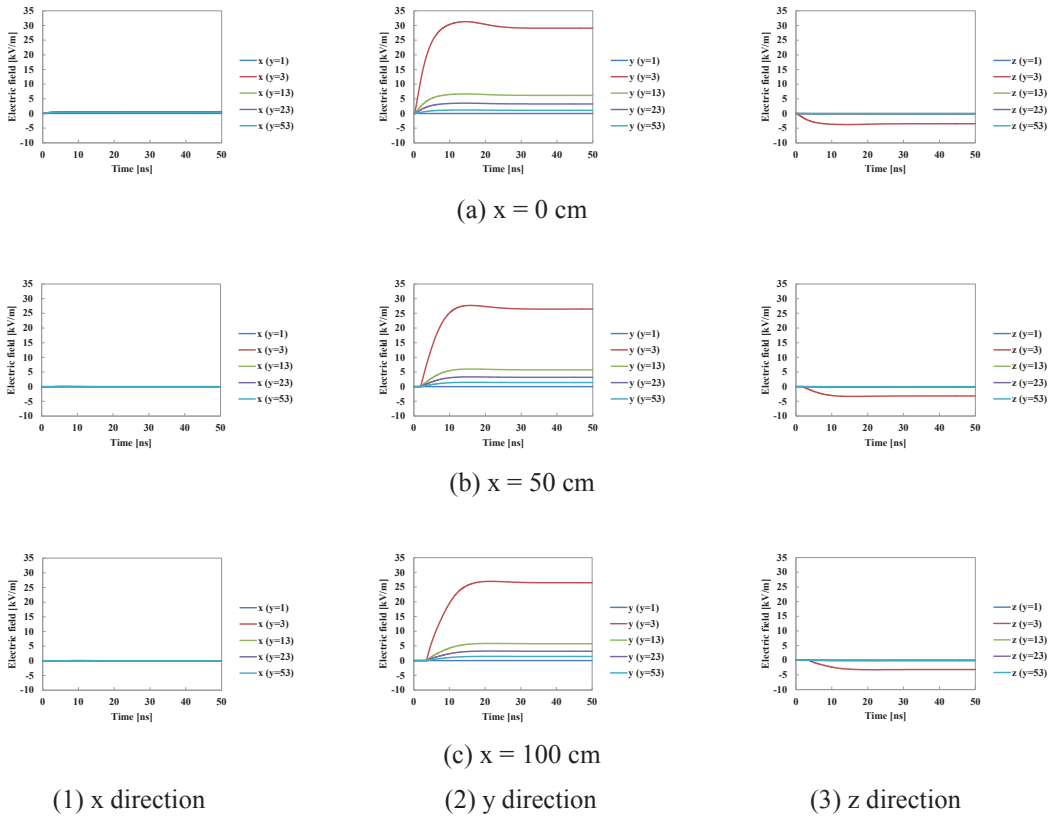
(a) x = 0 cm

(b) x = 50 cm

(c) x = 100 cm

(1) x direction   (2) y direction   (3) z direction

Fig. 7. Transient response of electric field intensity at various position : Case 1

(a) x = 0 cm

(b) x = 50 cm

(c) x = 100 cm

(1) x direction   (2) y direction   (3) z direction

Fig. 8. Transient response of magnetic field intensity at various position : Case 1

(a) x = 0 cm

(b) x = 50 cm

(c) x = 100 cm

(1) x direction   (2) y direction   (3) z direction
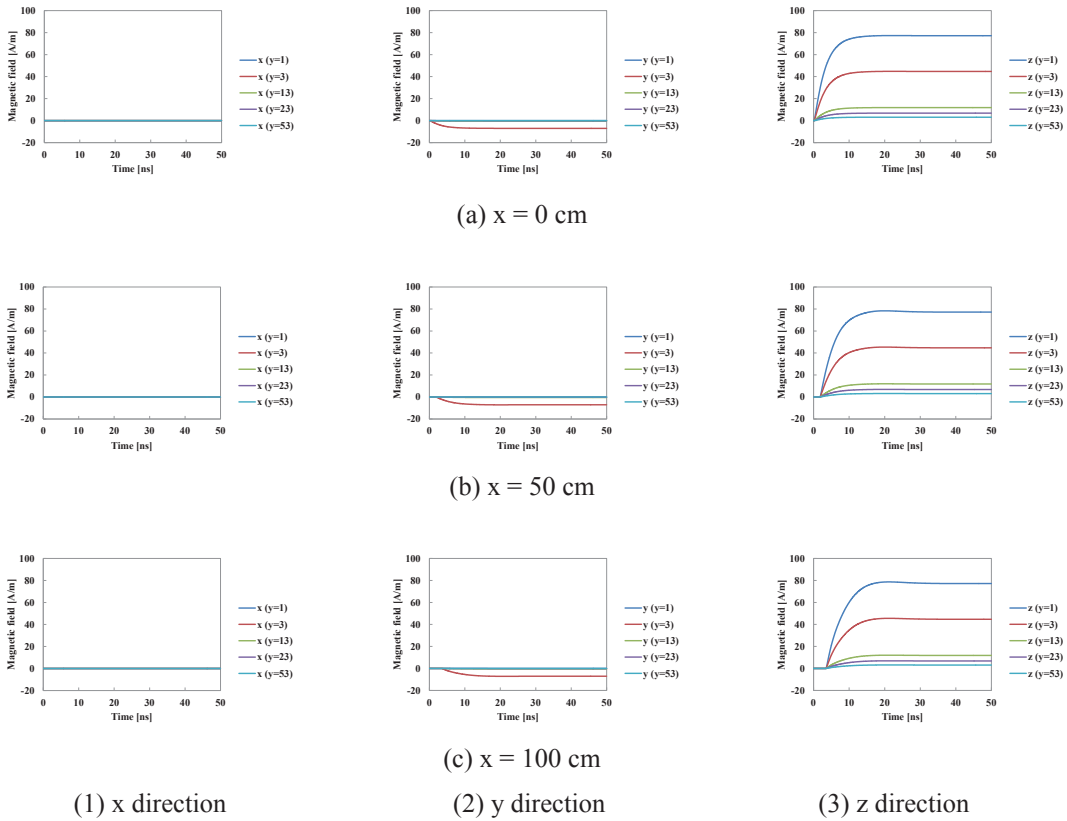
Fig. 9. Transient response of electric field intensity at various position : Case 2

space is the TEM mode.
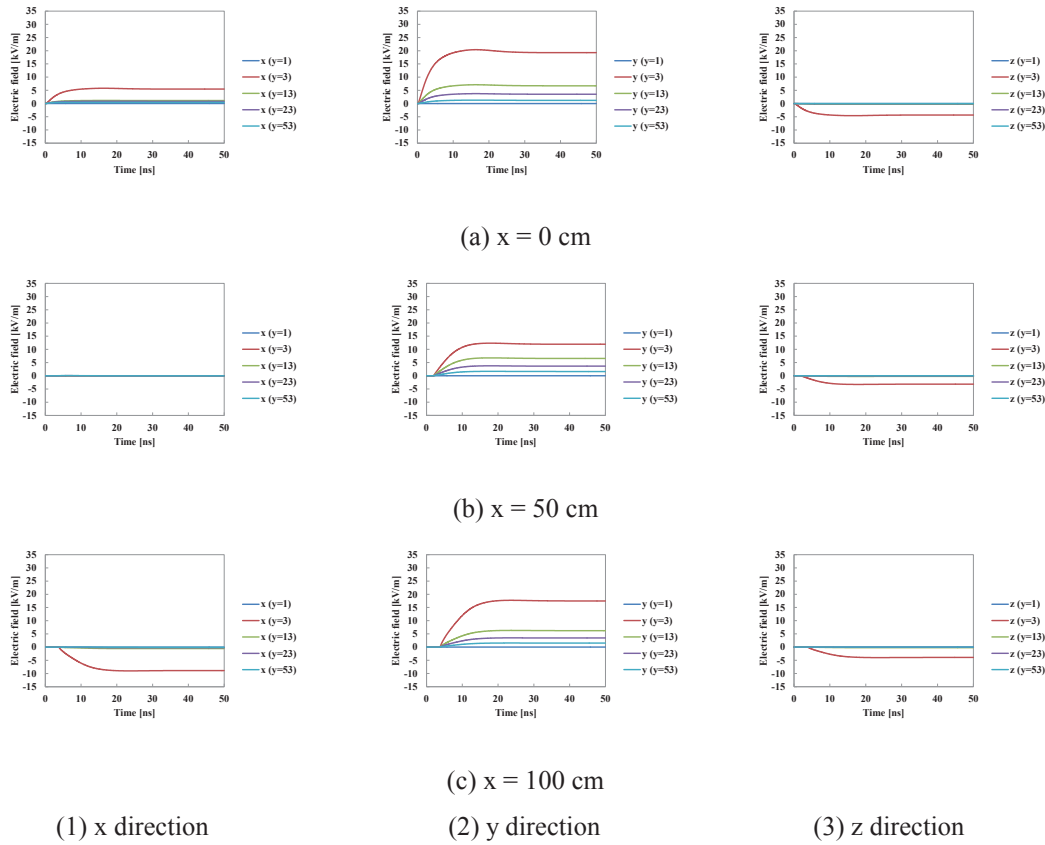
The above observation is confirmed in Fig. 8 where magnetic field intensity H_x for the longitudinal directim is zero. $E_x = 0$ in Fig. 7 is due to the perfect conductor assumption ($\rho_c = 0$) for the conductor in the FDTD simulation.

When the relative permittivity ε_i is 3 different from that of the air, E_x for x = 0 and y = 0 is not zero as observed in Fig.9, and this indicates possibility of TM mode at the sending end. Currents, voltages and magnetic field show nearly the same as those in Figs.6 and 8 in the case of $\varepsilon_i = 1$.

3.2.2. Above perfectly conducting earth :
Case 3 and 4

Figs.10 to 12 show the transient responses of voltages, currents, electric and magnetic field intensities, when a conductor is above a perfectly conducting earth
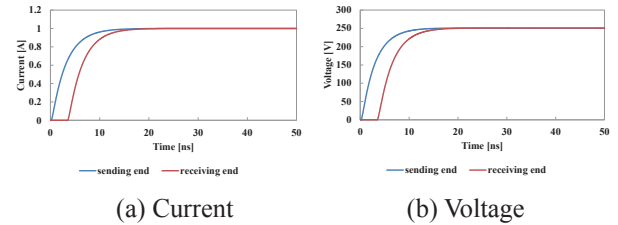

(a) Current   (b) Voltage

Fig. 10. Voltage and current : Case 3

with the relative permittivity $\varepsilon_i = 1$ of the conductor outer insulator (Case 3). It is observed that the waveforms of the voltages and the electric field intensities are smoothly and monotoneously increasing in comparison with those in a free space (Case 1). All the waveforms show a TEM mode propagation.

When the relative permittivity ε_i of the conductor outer insulator is 3 (Case 4), no significant difference of voltages, currents and magnetic intensities from those in the case of $\varepsilon_i = 1$ is observed. Fig.13 shows the electric field intensities. E_x at x = 0 is not zero which differs
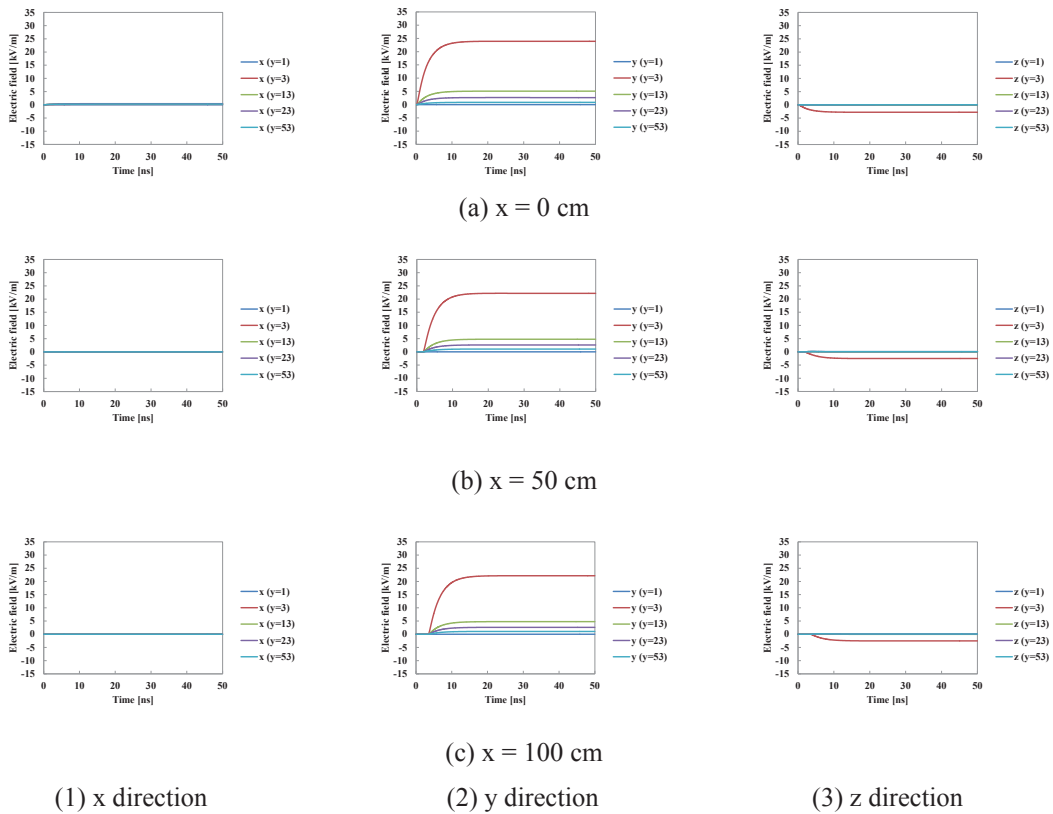
(a) x = 0 cm

(b) x = 50 cm

(c) x = 100 cm

(1) x direction   (2) y direction   (3) z direction

Fig. 11. Transient response of electric field intensity at various position : Case 3

(a) x = 0 cm

(b) x = 50 cm

(c) x = 100 cm

(1) x direction   (2) y direction   (3) z direction

Fig. 12. Transient response of magnetic field intensity at various position : Case 3

(a) x = 0 cm

(b) x = 50 cm

(c) x = 100 cm

(1) x direction　　　　　　　　(2) y direction　　　　　　　　(3) z direction
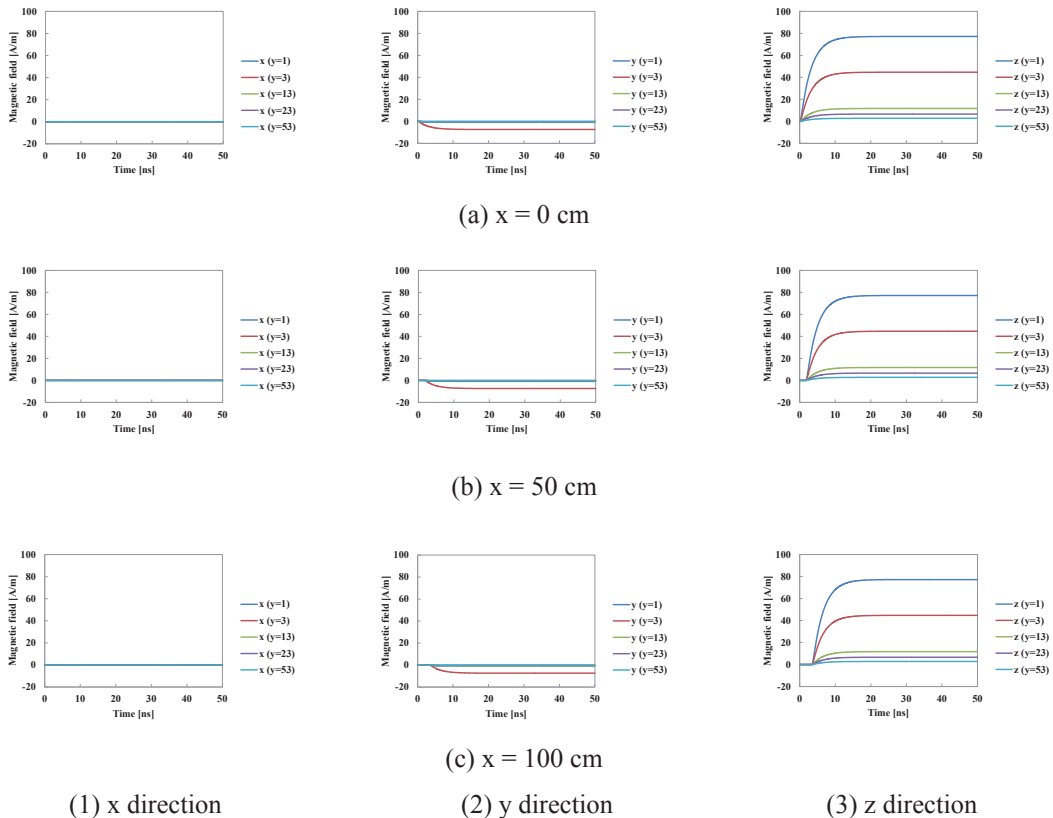
Fig. 13. Transient response of electric field intensity at various position : Case 2

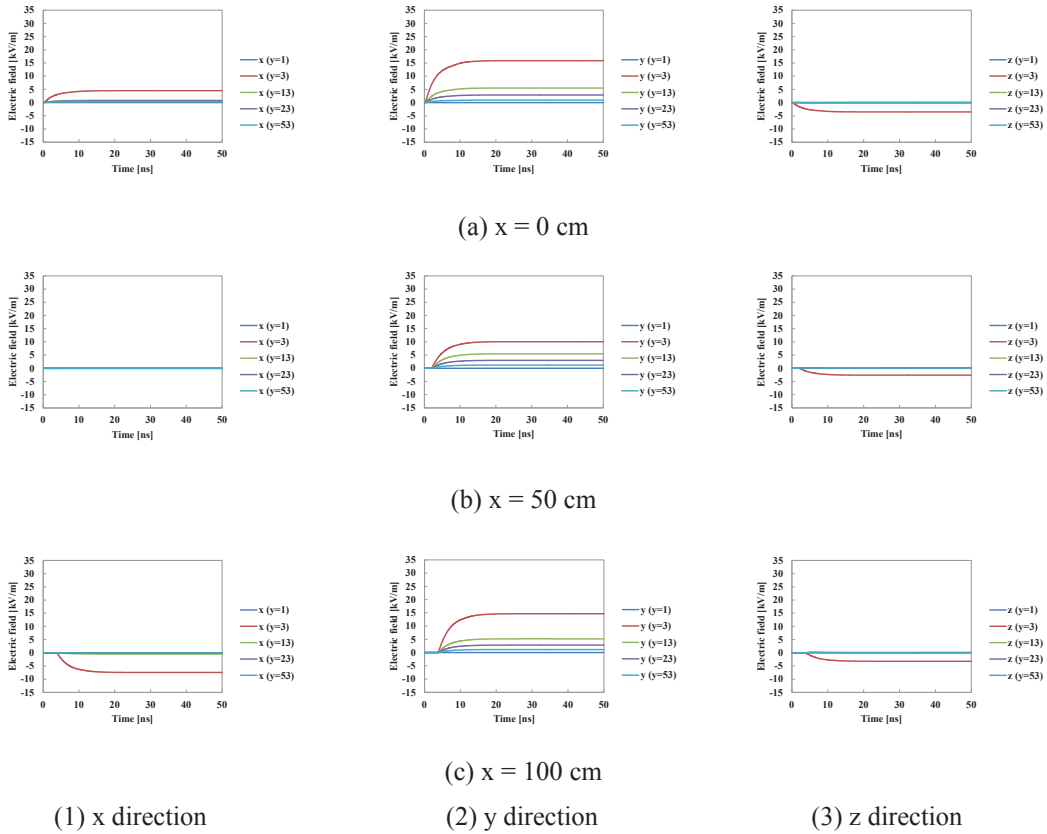from that for $\varepsilon_i = 1$ and indicates TM mode propagation.

3.2.3.　Above lossy earth : Case 5 and 6

Figs.14 to 16 show transient responses when a conductor with the relative permittivity $\varepsilon_i = 1$ is above a lossy earth (Case 5). The earth resistivity and relative permittivity are 100 Ωm and 1 respetively. The voltage and current waveforms at the receiving end (x = 100 cm) are observed to be distorted. E_x and H_x are zero. Thus, the wave propagation is estimated to be a TM mode.

Fig.17 shows the electric field intensities. It is observed that E_x is not zero, and thus the wave propagation is a TM mode.

When the relative earth permittivity ε_r is changed to 10, no significant difference is observed from those for $\varepsilon_r = 1$. Thus, it can be said that the earth permittivity does not affect the propagation mode.
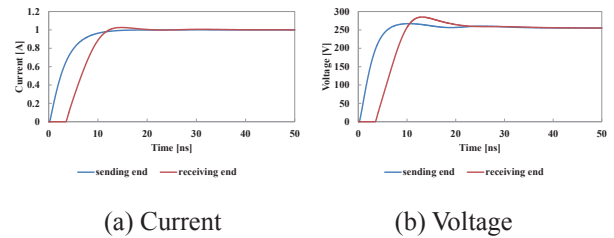

(a) Current　　　　　　　　(b) Voltage

Fig. 14. Voltage and current : Case 5

When the earth resistivity is taken to be 2000 Ωm, no significant difference from those in the case of 100 Ωm is observed. Therefore, it seems that the earth resistivity does not affect the propagation mode.

3.2.4.　Effect of the rise time T_f of applied current

When the rise time T_f of an applied current is changed to 1ns, i.e. the frequency involved in a transient is higher by 10 times than that in the case of $T_f = 10$ns, TM mode propagation at the sending end the receiving ends becomes more noticeable as expected.
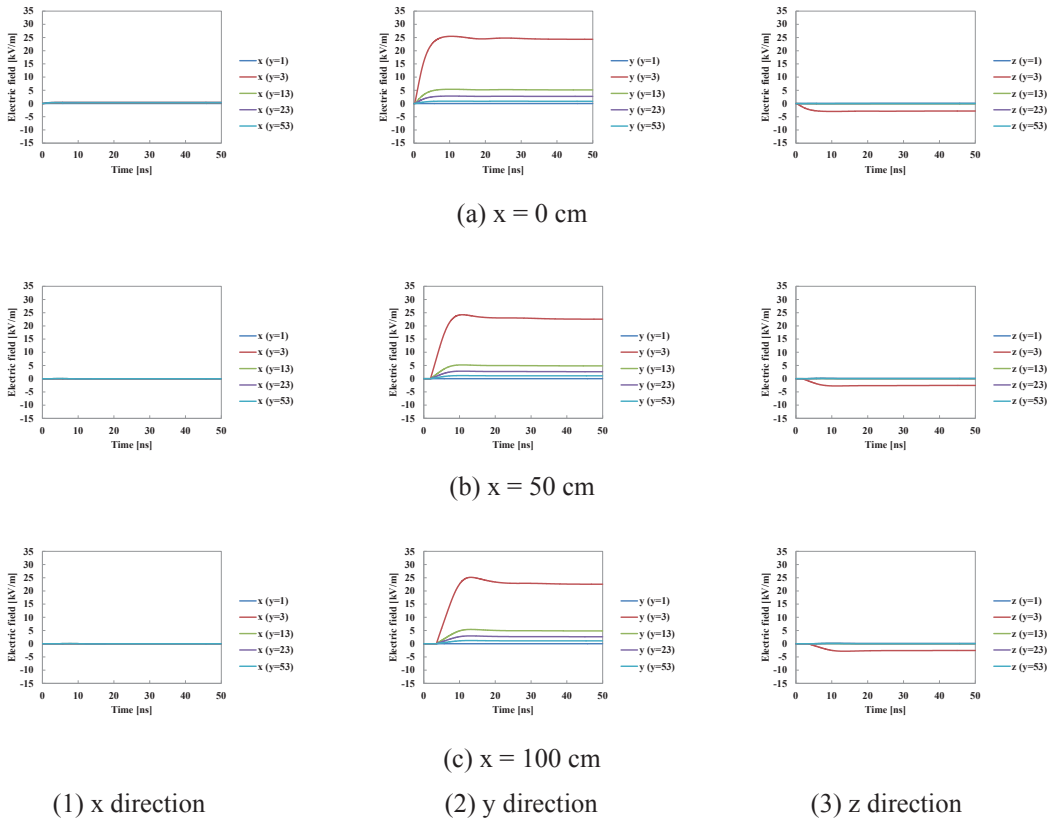
(a) x = 0 cm

(b) x = 50 cm

(c) x = 100 cm

(1) x direction   (2) y direction   (3) z direction

Fig. 15. Transient response of electric field intensity at various position : Case 5

(a) x = 0 cm

(b) x = 50 cm

(c) x = 100 cm

(1) x direction   (2) y direction   (3) z direction

Fig. 16. Transient response of magnetic field intensity at various position : Case 5

(b) x = 50 cm

(c) x = 100 cm

(1) x direction   (2) y direction   (3) z direction
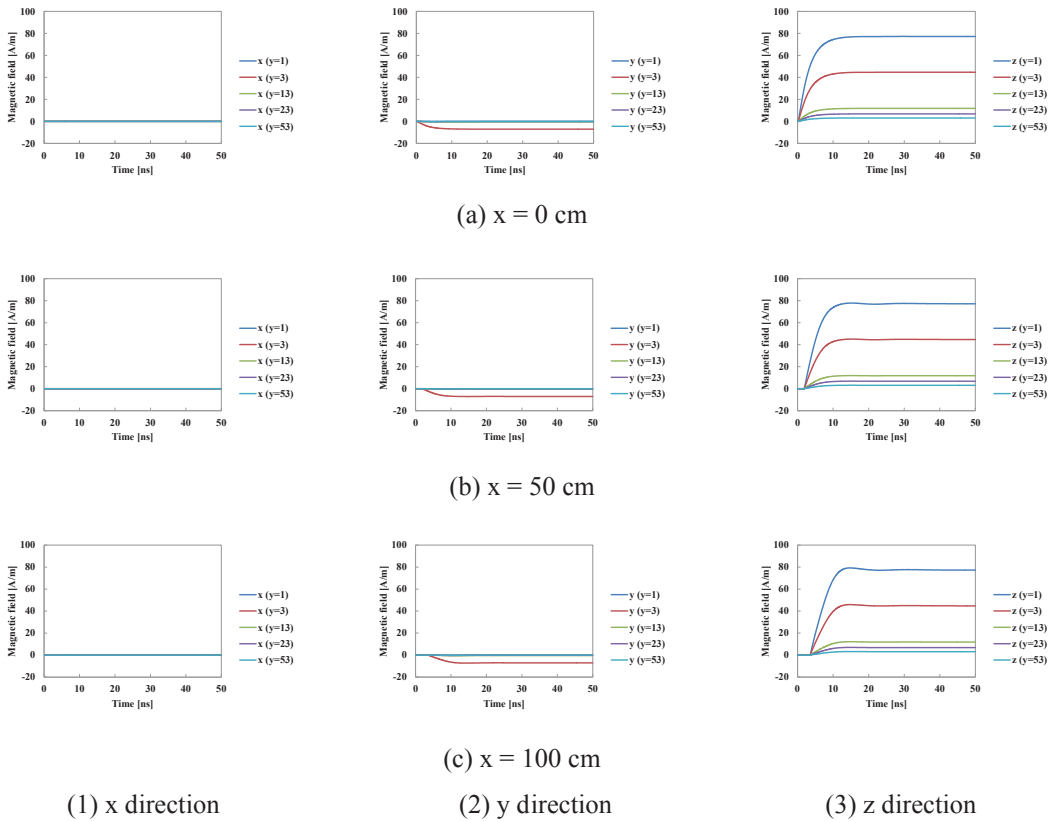
Fig. 17. Transient response of electric field intensity at various position : Case 6

4. Conclusions

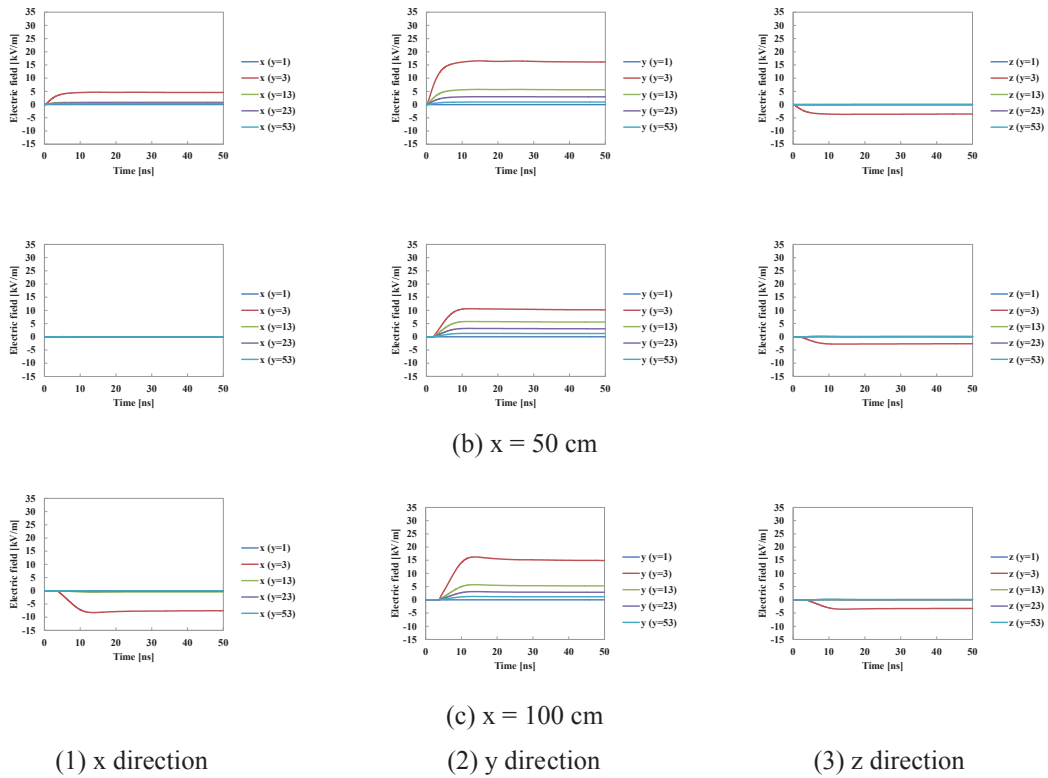Transition of TEM and TM modes on an overhead bare conductor pointed out by Kikuchi has been confirmed in a frequency-domain analysis by adopting an accurate earth-return impedance and Wires admittance.

FDTD simulations of transient currents and voltages have been carried out to investigate the TEM and TM / TE modes of propagation on a conductor covered by an insulator with the relative permittivity being unity and other than unity in a free space, above perfectly conducting earth and above a lossy earth when a step-like current is applied at the sending end of the conductor. The transition between the TEM and TM modes are observed at the sending and receiving ends when the relative permittivity of the outer insulator being other than unity. However, when the permittivity is the same as that of a free space (air), no transition is observed. The result differs from that observed in a frequency domain by Kikuchi and by the authors in this paper.

One of the reasons of the above difference is estimated due to the fact that the frequency-domain analysis assumes an infinitely long homogenous conductor which is a conventional assumption in any circuit theory. The infinitely long conductor cannot be simulated by the FDTD method. This requires a further investigation together with FDTD parameters.

Reference

1) F. Pollaczek, "Über das Feld einer unendlich langen wechselstrom-durchlossen einfachleitung," *E.N.T.*, **3**[9], 339–359 (1926).

2) J. R. Carson, "Wave Propagation in Overhead Wires with Ground Return," *Bell Syst. Tech. J.*, **5**, 539–554 (1926).

3) E. D. Sunde, Earth Conduction Effects in Transmission Systems, (Dover Publications, Inc., New York, 1968), pp.1-373.

4) W. H. Wise, "Propagation of High-frequency Currents in

Ground Return Circuits," *Proc. I. R. E.*, **22**[4], 522–527 (1934).

5) W. H. Wise, "Potential Coefficients for Ground Return Circuits," *Bell Syst. Tech. J.*, **27**, 365–371 (1948).

6) H. Kikuchi, "Wave Propagation on the Ground Return Circuit in High Frequency Regions," *J. IEE Japan*, **75**[805], 1176–1187 (1955).

7) H. Kikuchi, "Electro-magnetic Field on Infinite Wire at High Frequencies above Plane-earth," *J. IEE Japan*, **77**[825], 721–733 (1957).

8) G. Goubau, "Surface Wave and Their Application to Transmission Lines," *J. A. Physics*, **21**[11], 1119–1128 (1950).

9) G. Goubau, "Single-conductor Surface Wave Transmission Lines," *Proc. I. R. E*, **39**[6], 619–624 (1951).

10) A. Sommerfeld, "Fortpflanzung elektrodynamischer Wellen an einem zylindrischen Leiter," *Ann. Phys. u. Chemie*, **67**, 233, Dec. 1899 (See J. A. Stratton, "Electromagnetic Theory," McGraw-Hill Book Co., New York, pp. 527, 1941).

11) M. Nakagawa, A. Ametani and K. Iwamoto, "Further Studies on Wave Propagation in Overhead Lines with Earth Return: Impedance of Stratified Earth," *Proc. IEE*, **120**[12], 1521–1528 (1973).

12) A. Ametani, "Stratified Earth Effects on Wave Propagation – Frequency-dependent Parameters –," *IEEE Trans. Power Apparatus and Systems*, **93**[5], 1233–1239 (1974)

13) M. Nakagawa, "Admittance Correction Effects of a Single Overhead Line," *IEEE Trans. Power Apparatus and Systems*, **100**[3], 1154–1161 (1981)

14) VSTL:http://criepi.denken.or.jp/jp/electric/facilitySoft/ software_02.html

Appendix: Earth-return impedance and admittance

A1. Stratified-earth impedance

The earth-return impedance of a three-layer earth illustrated in Fig. 1 is given in the following form [12].

$$Z_{ij} = j\omega(\mu_0/2\pi)(P_0 + Q' - jR') \tag{A.1}$$

$$Q' - jR' = 2\int_0^\infty A_3 \cdot F(s) \cdot ds \tag{A.2}$$

$$P_0 = \ell n(D_{ij}/d_{ij}), F(s) = \exp\{-(h_i + h_j)s\}\cdot\cos(ys) \tag{A.3}$$

where $d_{ij} = \sqrt{y^2 + (h_i - h_j)^2}$, $D_{ij} = \sqrt{y^2 + (h_i + h_j)^2}$

$$A_3 = (c_1 + c_2)/\{(s + \mu_0 b_1)c_1 + (s - \mu_0 b_1)c_2\} \tag{A.4}$$

$$c_1 = (b_1 + b_2)(b_2 + b_3) + (b_1 - b_2)(b_2 - b_3)\exp\{2a_2(d_1 - d_2)\}$$

$$c_2 = [(b_1 - b_2)(b_2 + b_3) + (b_1 + b_2)(b_2 - b_3)\exp\{2a_2(d_1 - d_2)\}]\exp(-2a_1 d_1)$$

$$a_k = \sqrt{s^2 + m_k^2 - m_0^2}, \ b_k = a_k/\mu_k \quad (k = 1, 2 \text{ and } 3)$$

$$m_0^2 = j\omega\mu_0(\sigma_0 + j\omega\varepsilon_0), m_k^2 = j\omega\mu_k(\sigma_k + j\omega\varepsilon_k) \tag{A.5}$$

$\mu_k, \sigma_k, \varepsilon_k$: permeability, conductivity and permittivity of medium k

μ_0, ε_0 : for free space (air)

The first term in (A.1) is the inductance due to the geometry of the conductor. The second term is the earth-return impedance of an infinite conductor above the three-layer earth.

When d_2 in Fig. 1 becomes infinity, i.e. two-layer earth, A_3 can be reduced to A_2.

$$A_2 = \frac{b_1 + b_2 + (b_1 - b_2)\exp(-2a_1 d_1)}{(s + \mu_0 b_1)(b_1 + b_2) + (s - \mu_0 b_1)(b_1 - b_2)\exp(-2a_1 d_1)} \tag{A.6}$$

If the earth is homogeneous, i.e. $d_1 = \infty$, the above equation reduces to

$$A_1 = (s + \mu_0 b_1)^{-1} = 1/\left\{s + (\mu_0/\mu_1)\sqrt{s^2 + m_1^2 - m_0^2}\right\} \tag{A.7}$$

In general, the earth permittivity μ_e is the same as that of free space, i. e. $\mu_e = \mu_0$. Then $Q'-jR'$ of (A.2) is rewritten by:

$$Q' - jR' = 2\int_0^\infty F(s)/(a + s)ds \tag{A.8}$$

where $a = \sqrt{s^2 + m_1^2 - m_0^2}$, $m_1^2 = j\omega\mu_e(\sigma_e + j\omega\varepsilon_e)$ (A.9)

A2. Earth-return admittance

Wise's formula of the earth-return admittance is given in the following form [5] which is the same as that derived by Nakagawa [13].

$$[Y] = j\omega[C], [C] = [P]^{-1}, P_{ij} = (P_0 + M + jN)/2\pi\varepsilon_0 \tag{A.10}$$

$$M + jN = 2\int_0^\infty (A + jB)ds, \ A + jB = F(s)/(a + bs) \tag{A.11}$$

$$b = m_1^2/m_0^2 = (\sigma_e + j\omega\varepsilon_e)/j\omega\varepsilon_0 \tag{A.12}$$

for $\mu_e = \mu_0$, $F(s)$ in (A.3), a in (A.9)

A3. Carson's, Pollaczek's and Sunde's Formulas

It is well-known that Carson's earth-return impedance [2] is given in the following form, which is the same as Pollaczek's formula [1].

$$Z_{cij} = j\omega(\mu_0/2\pi)\left[\ell n(D_{ij}/d_{ij}) + (2/j)(P + jQ)\right] \quad \text{(A.13)}$$

$$P + jQ = \int_0^\infty \left(\sqrt{s^2 + j} - s\right)\cdot \exp\left\{-\left(h_i^{'} + h_j^{'}\right)s\right\}\cdot \cos(y'\!\cdot\!s)\cdot ds \quad \text{(A.14)}$$

where $h' = \sqrt{\alpha}\,h$, $y' = \sqrt{\alpha}\cdot y$, $\alpha = j\omega\mu_0\sigma_e$.
Equation (A.14) is rewritten considering α as follows:

$$P + jQ = j\int_0^\infty \left[F(s)/\left(\sqrt{s^2 + j\alpha} + s\right)\right]\cdot ds \ .$$

Then, (A.13) is written in the following form.

$$Z_{cij} = j\omega(\mu_0/2\pi)\left[P_0 + (Q_c - jR_c)\right] \quad \text{(A.15)}$$

$$Q_c - jR_c = 2\int_0^\infty A_c\cdot F(s)\cdot ds \,, \ A_c = 1/(a_c + s) \quad \text{(A.16)}$$

where $a_c = \sqrt{s^2 + j\omega\mu_0\sigma_e}$ and $Q_c = 2Q$, $R_c = 2P$ (A.17)

Because the earth permittivity ε_e is not included in the above equations, it has been said that Carson's impedance formula cannot deal with displacement currents.

The impedance formulas described in Section A1 can handle the displacement currents. When the earth permeability and permittivity are the same as those in free space, i. e. $\mu_e = \mu_0$ and $\varepsilon_e = \varepsilon_0$, (A.9) is simplified as:

$$a = \sqrt{s^2 + j\omega\mu_0\sigma_e} \,, \ m_1^2 = j\omega\mu_0(\sigma_e + j\omega\varepsilon_0).$$

The above equation is the same as Carson's one in (A.17).

Now, it should be clear that Carson's and Pollaczek's formulas in (A.13) to (A.17) are specific to the condition of $\varepsilon_e = \varepsilon_0$. The formulas can deal with the displacement currents under the condition of $\varepsilon_e = \varepsilon_0$.

Sunde also derived the earth-return impedance of wires with infinite length above the earth surface [3]. His formula is the same as that by Carson in (A.16) except "α", i.e.

$$\alpha_s = \sqrt{s^2 + j\omega\mu_0(\sigma_e + j\omega\varepsilon_e)} \quad \text{(A.18)}$$

It is noteworthy that Wise tried to modify Carson's formula so as to be able to deal with the displacement currents for arbitrary ε_e in a high frequency region, and derived the following equation [4].

$$a_w = \sqrt{s^2 + j\omega\mu_0\{\sigma_e + j\omega\varepsilon_0(\varepsilon_r - 1)\}} \quad \text{(A.19)}$$

where $\varepsilon_e = \varepsilon_r\varepsilon_0$.

Replacing μ_e and ε_e in (A.9) by μ_0 and $\varepsilon_r\varepsilon_0$, the above Wise's high frequency formula is obtained. Equations (A.9) and (A.19) have shown that Sunde's formula in (A.18) involves an error. The error is corrected by replacing ε_e in (A.18) by $\varepsilon_0(\varepsilon_r - 1)$ as

in (A.19). Now, it appears that modified Pollaczek's, Carson's and Sunde's formulas are identical to each other and are given by (A.9) and (A.19).

Kikuchi's formulas of earth-return impedance and admittance were given in an iterative form. Assuming that the initial condition of propagation constant Γ_0 for the first iteration is :

$$\Gamma_0 = j\beta_0 = j\omega\sqrt{\varepsilon_0\mu_0} \quad \text{(A.20)}$$

then, the impedance formula agrees with (A.1), (A.7) and (A.8), and the admittance formula agrees with Wise's one.